Bull. Mater. Sci., Vol. 34, No. 7, December 2011, pp. 1599–1604. © Indian Academy of Sciences.

Synthesis and *in situ* mechanism of nuclei growth of layered double hydroxides

H S PANDA, R SRIVASTAVA† and D BAHADUR*

Department of Metallurgical Engineering and Materials Science, †School of Biosciences and Bioengineering, Indian Institute of Technology Bombay, Mumbai 400 076, India

MS received 6 December 2009

Abstract. **A host–guest material such as layered double hydroxide (LDH) has generated immense interest in current research due to its technological importance, whereby its dimension significantly affect its mechanical and other physical properties. The purpose of this study was to prepare Mg/Al-LDHs by systematically varying the molar concentration of cations, aging time and pH. The prepared LDHs were characterized by powder X-ray diffraction, Fourier transform infrared spectroscopy, thermal analysis and transmission electron microscopy to confirm their formation and morphology. We qualitatively observed a new growth route for LDH system which is dissimilar to the existing growth mechanism. The rate of growth is shown to be slower than the well known Ostwald ripening process. This unusual behaviour is due to the formation of effective passivation layer by Na^+ ions around the generated LDHs nuclei. This suggested growth mechanism will be helpful in further controlling the particle size of other LDH, which may be useful for various future applications.**

Keywords. **LDHs; growth mechanism; morphology.**

1. Introduction

Over the past decade, layered double hydroxides (LDHs), otherwise named as hydrotalcites have attracted attention of the researchers due to their layered structure and their high anion exchange capacity, which make them potential candidature for technical applications in various domains, such as medicine, catalysis, separation technology, polymer reinforcement, electrochemistry, etc. (Adams 1987; Fogg *et al* 1999; Khan *et al* 2001; Kwak *et al* 2004; Li *et al* 2005a; Zhang *et al* 2005; Panda *et al* 2009). The structure of LDHs can be described from brucite-type $Mg(OH)_2$, where metal ions are situated at the centre of the octahedron and the vertices are occupied by hydroxide ions. The positive charge is generated by partial substitution of divalent metal cations by trivalent ones within the brucite-like layers and is balanced by an equal negative charge from the inter layer solvated anions (Lakraimi *et al* 2000). The general formula for LDH is $M^{II}_{1-x}M^{III}_{x}(OH)_2(Y^{n-})_{x/n}\cdot mH_2O$, where $x = 0{\cdot}2–0{\cdot}33$, $m = 1 - 3Y/2$, M^{II} = divalent cations, M^{III} = trivalent cations and Y^{n-} = n-valent anions (Kaneyoshi and Jones 1999). A large number of such compounds are known, and one of their important features is the relative ease of synthesis of a range of LDH matrices with a significant variation of layer charge, the concentration of the reactants in the reaction medium and the synthesis procedures. The influence of the M^{II} and M^{III} salts, the M^{II}/M^{III} ratio and the interlayer anion on the crystallinity and morphology of the co-precipitated LDHs have been widely studied in the literature cited previously (Franklin *et al* 1995; Chang *et al* 2005).

Controlling the particle size of LDHs is a challenge, as it is important for many potential applications. For example, nanodimension LDHs particles can be used as additives in agricultural plastic film since their infrared absorbing properties enhance the heat retaining properties of the film (Hancock 1990; Adachi-Pagano *et al* 2003). Also, the dimension of the particle plays a significant role in retaining the mechanical and other physical properties of polymers. Aluminum-substituted LDHs compounds are important because of their stability and high electrochemical performance. The effect of electrochemical behaviour on crystallite size of a nickel-metal hydride electrode was analysed by mathematical model, which clearly showed that the crystallite size significantly affects the electrode performance. Recent experimental findings (Hu and Lei 2007) show that the crystallite size of the sample has evident effects on its discharge capacity at high current density. Several articles (Ennadi *et al* 2000; Prevot *et al* 2001; We *et al* 2005; Panda *et al* 2008b, 2009) have been published so far on LDHs containing intercalated anion. But the lack of literature on the growth parameters of LDHs during synthesis and its conviction that the growth of nano LDHs occurs via the Ostwald ripening behaviour, despite experimental verifi-

*Author for correspondence (dhirenb@iitb.ac.in)

cation of different constraints used in synthesis, are absent. Different synthesis techniques have been developed so far to control the particle size, but the co-precipitation route is one of the most preferred routes to synthesize M^{II}/M^{III} LDHs. Recent theoretical investigation (Talapin *et al* 2001) on the growth of nanocrystals suggest that the growth could be either controlled by diffusion of the particles, i.e. Ostwald ripening, or controlled by the reaction at the surface, or by both parameters even in the absence of capping agent. In these cases the nano LDHs growth after nucleation in absence of any capping agent is the most logical ground for inquiring the growth kinetics.

In this work we have synthesized Mg/Al-CO_3 LDHs systems by varying the molar concentration of metal ions. For a particular metal ion concentration, we qualitatively investigated the growth behaviour of nanocrystals upon varying the synthesis parameters. In our studies we noticed some novel features; the growth of LDHs crystals can be strongly affected by the reactant itself and the growth model (figure 1) is qualitatively different compared to that of the universally accepted Ostwald ripening process. To investigate the *in situ* particles growth, there are no suitable techniques available, although transmission electron microscope (TEM) is the most suitable technique to determine the average particle size and size distribution *ex situ*, but due to high agglomeration tendency of LDHs particles, it is restricted to observe individual particles during measurement and it may therefore agglomerate or fold the layered platelets. In this context, the average crystallite size was calculated from background subtracted X-ray diffraction (XRD) patterns by using Scherrer formula. The FWHM was calculated by fitting Gaussian on the XRD patterns through Origin software. Finally, the morphology of LDHs particles was compared using TEM data.

2. Experimental

Magnesium nitrate hexahydrate was obtained from Fluka with 99% purity. Aluminium nitrate nonahydrate (98%), sodium carbonate (99%) and sodium hydroxide were obtained from Thomas Beaker Chemicals Limited. LDHs having carbonate as interlayer anion with Mg and Al as the octahedral cations (designed MgAl-CO_3) were prepared using an established method (Whilton *et al* 1997). Salt solutions with molar ratios of 2 : 1, 3 : 1 and 4 : 1 were prepared by adding $Mg(NO_3)_2{\cdot}6H_2O$ (2·2, 3·3 and 4·4 mmol) and $Al(NO_3)_3{\cdot}9H_2O$ (1·1 mmol) in 18 ml de-ionized water. After complete dissolution, the above solution was added drop wise to a vigorously stirred Na_2CO_3 solution in 60 ml de-ionized water. Freshly prepared 1 M NaOH solution was then added drop wise to the above solution to maintain constant pH (~ 11). The resultant gel was aged by stirring at 65°C for 12 h. The precipitate was separated from the solution by centrifugation, washed several times with de-ionized water and dried in vacuum. All these reactions were carried out in an inert atmosphere.

In order to study the effect of synthesis parameters, initially the synthesis process was repeated for pH 9, pH 10 and pH 11 keeping all other parameters constant, while at pH 11, the above reactions are studied at different aging time. Additionally, for investigating the effect of sodium hydroxide concentration on growth at particular pH, aging time, aging temperature and metal ion concentration, particles are nucleated in various molar concentration of NaOH. Powder X-ray diffraction (PXRD) data was collected on a Phillips PW 3040/60 diffractometer using Cu-Kα radiation (λ = 1·5406 Å) with scan step time 0·017 s. All measurements were made using a generator voltage 40 kV and emission current of 30 mA. The characteristic bonding nature between CO_3^{2-} and metal hydroxides was confirmed through Fourier transform infrared spectra (FT–IR) and back up of the layered structure was observed through thermal analysis (SDT Q600). TEM images were taken on a Phillips-CM200 electron microscope operated at 200 kV wherein one drop of suspended samples (solvent–ethanol) was deposited on carbon coated copper grid and dried and images obtained.

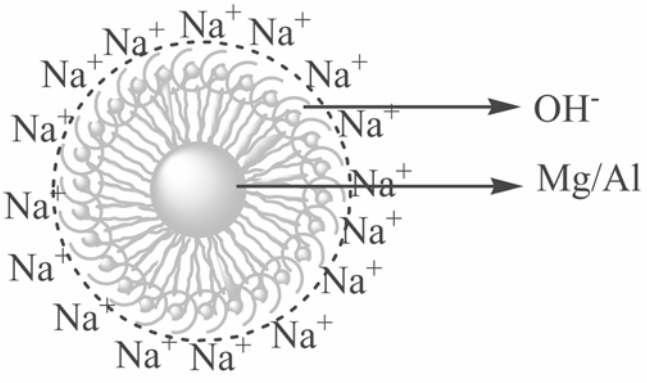

Figure 1. Schematic representation of *in situ* Na^+ passivation layer around the LDHs nuclei.

3. Results and discussion

X-ray diffraction patterns presented in figure 2 show that well-crystallized hydrotalcite-like compounds are obtained and no other phase is identified. The X-ray diffraction for these samples typically consist of anionic clay having molecular formula $Mg_6Al_2(OH)_{16}CO_3{\cdot}4H_2O$ with carbonate in the interlayer space. The sharp peak obtained at d = 7·69 Å (2θ = 11·5°) can be ascribed to (003) (*hkl*) of a hydrotalcite structure with rhombohedral 3R packing of the layers. Upon considering the thickness of brucite layer, i.e. 4·8 Å (Whilton *et al* 1997), the gallery spacings are approximately 2·89, 3·06 and 3·16 Å for 2 : 1, 3 : 1 and 4 : 1 molar ratio, respectively. The interlayer space

calculated is 2·89 Å, indicating that carbonate anions are located with their molecular plane parallel to the brucite-like layers (Zhao *et al* 2002). Assuming the 3R packing of the layers, lattice parameter c corresponds to three times the value of d (003), i.e. $c = 23{\cdot}07$ Å and this is the distance between the center of one layer to the center of other layer. Lattice parameter a corresponds to the average closest metal–metal distance within a layer, and is calculated as twice the position of the diffraction maximum due to planes (110), i.e. $a = 3{\cdot}04$ Å for Mg : Al ratio of 2 : 1. Further, it increases with the increasing Mg content on the brucite-like layers, as the ionic radius for Mg^{2+} (0·065 nm) is larger than that for Al^{3+} (0·050 nm). The average crystallite size in the a and c directions may be calculated from the values of the FWHM of the (110) and (003) diffraction peaks, respectively, and by using the Scherrer formula, i.e. $L = 0{\cdot}89\lambda/(\beta(\theta) \times \cos\theta)$, where L is the crystallite size, λ the wavelength of the radiation used, θ is the Bragg diffraction angle and $\beta(\theta)$ the FWHM (Li *et al* 2005b). In order to gain information on the mechanism of growth process, we plotted the crystallite size of the nano LDHs as a function of aging time at fixed temperature of 338 K, pH (11) and NaOH concentration (1 M) in figures 3 and 4. It is observed from this figure that the size of the growing nuclei depends strongly on the reaction time, which is the expected behaviour within the diffusion-limited Ostwald ripening process. To gain further insight into the mechanism of growth, we observed the crystallite size as a function of pH of the reaction medium during synthesis at fixed temperature (338 K), aging time (12 h) and sodium hydroxide concentration (1 M). It is evident from this study that the growth of crystallite size at a specific time depends on the reaction medium pH, where NaOH is the prime parameter to maintain the required pH. This can be explained by considering the hydroxyl ions in the solution, which promote the Ostwald ripening factor. As for higher pH, in the beginning sodium hydroxide solution was added in sodium carbonate solution to attain the required pH.

We have probed this unusual behaviour by carrying out different studies, systematically varying the sodium hydroxide concentration at different pH and keeping all other parameters constant (figure 5). Interestingly, we found that (table 1) the crystallites growth decreases with decreasing sodium hydroxide concentration. Additionally,

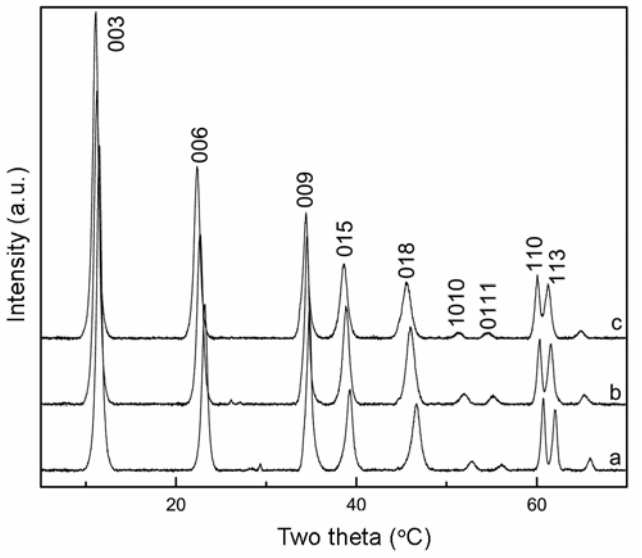

Figure 2. XRD patterns of Mg/Al-CO_3 LDHs having molar ratios: a. Mg/Al-2 : 1 (12 h), b. Mg/Al-3 : 1 (12 h) and c. Mg/Al-4 : 1 (12 h).

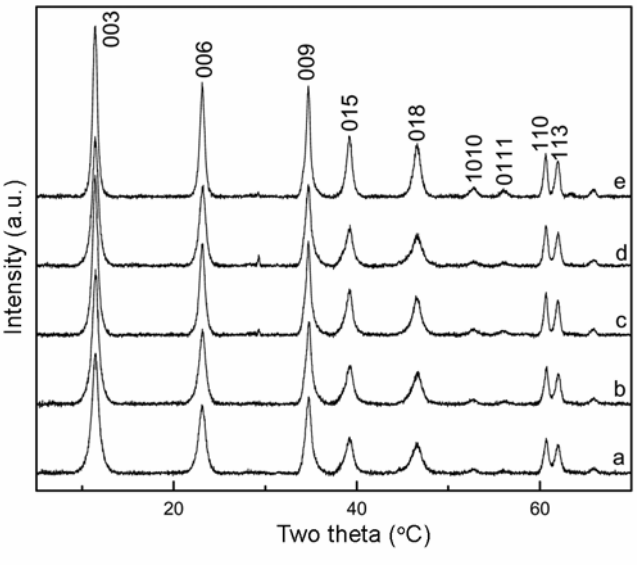

Figure 3. XRD patterns of Mg/Al-CO_3 LDHs with constant temperature (65°C) having aging time: a. 2 h, b. 6 h, c. 12 h, d. 18 h and e. 24 h.

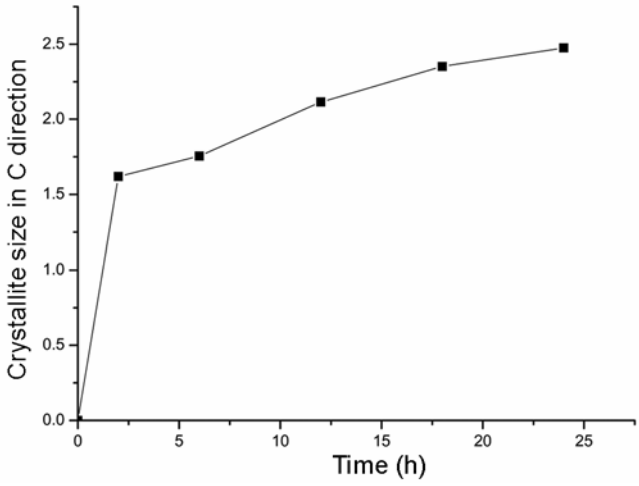

Figure 4. Variation of crystallite size as a function of aging time of Mg/Al-CO_3 LDHs.

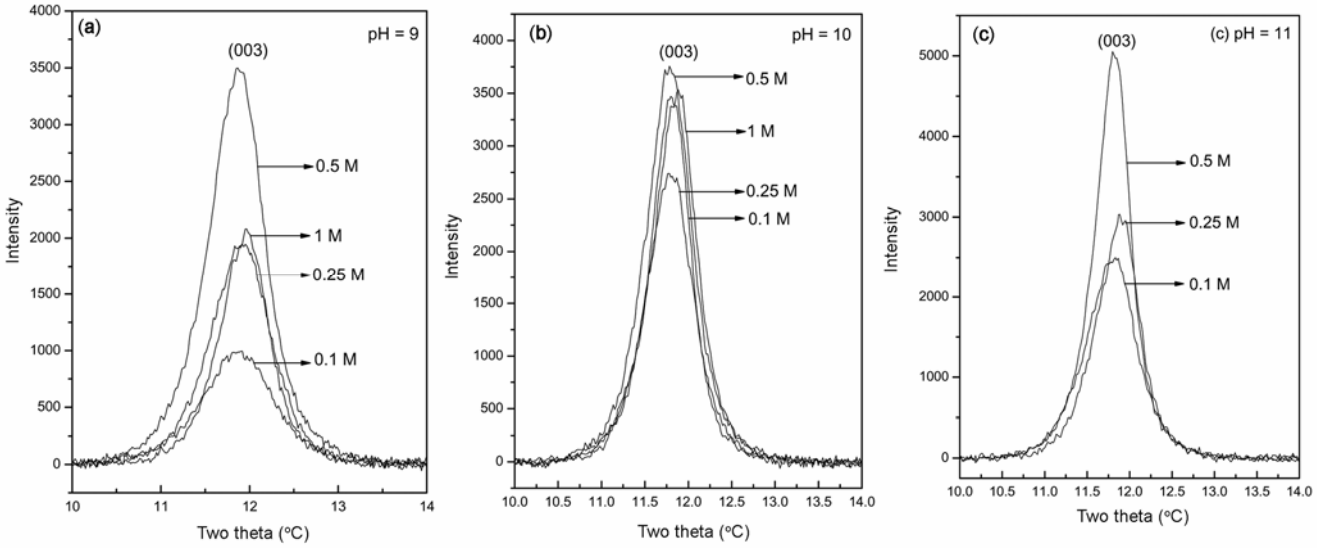

Figure 5. XRD patterns of Mg/Al-CO_3 LDHs at pH: (**a**) 9, (**b**) 10 and (**c**) 11 having different molar concentration of NaOH.

Table 1. Variation of crystallite size of Mg/Al-CO_3 LDHs having Mg/Al molar ratios 2.

Molar concentration of NaOH (M)	Average crystallite size		
	pH 9	pH 10	pH 11
1	2·42	2·57	–
0·5	2·08	2·45	3·1
0·25	1·65	2·43	2·59
0·1	1·97	2·85	2·24

we observe formation of nano LDHs in all the reactions is instantaneous and only the growth of the crystallites is affected by the presence of NaOH. As the growth rate was found to depend strongly on the amount of water present, the possibility of growth was excluded due to initial water taken for preparing sodium carbonate and salt solution, as it was same for all reaction medium. The initial decrease followed by a slow increase at higher concentration of NaOH suggests that the addition of base not only maintains the pH of the reaction medium but also supports the nuclei growth. Hence, the results in figure 5 point to a completion of two reaction parameters, where one parameter suppresses the other at a critical limit. It is important to note that for LDH, nucleation and growth are assisted by water. But, at constant water concentration, upon increasing the concentration of NaOH above a critical limit, it promotes the nuclei to grow. In order to get conformation of our hypothesis, the above process was repeated for other pHs keeping all the parameters constant (figures 5b and c). The same trend was observed in all the cases, indicating that hydroxyl or sodium ions of sodium hydroxide play a key role to control the particle size. In order to identify if hydroxyl or sodium or both ions take part in the growth process, we have made a logical argument. As we go on reducing the sodium hydroxide concentration, the overall solution concentration increases, as more amount of sodium hydroxide solution is required to maintain constant pH for a particular salt concentration. Such a behaviour is unusual, since one does not expect this retardation of growth process, as small amount of water (Viswanatha *et al* 2004) specifically increases the size of crystallites. This behaviour is observed below the critical concentration of NaOH (0·25 M). This suppression of crystal growth can be explained by using recently reported capping mechanism for zinc oxide nanocrystals (Viswanatha *et al* 2007), which is the reverse of the Ostwald ripening phenomenon. In the presence of sodium hydroxide, sodium ions adjoining the generated nuclei act as a capping agent and hinder the nucleating particles growth. As the hydroxyl ion attaches to the surface of the nano LDHs, it is noticeable that the sodium ion acts as a counter ion and hinders the other nucleating metal ion. From the table, it was noticed that at higher pH the critical limit point shifts to further lower concentration of sodium hydroxide. This might be due to the presence of excess sodium ions.

In order to further confirm the effect of sodium ion concentration on particles morphology, LDHs particles were characterized using TEM and it was observed that there is significant change of morphology at pH 9 with

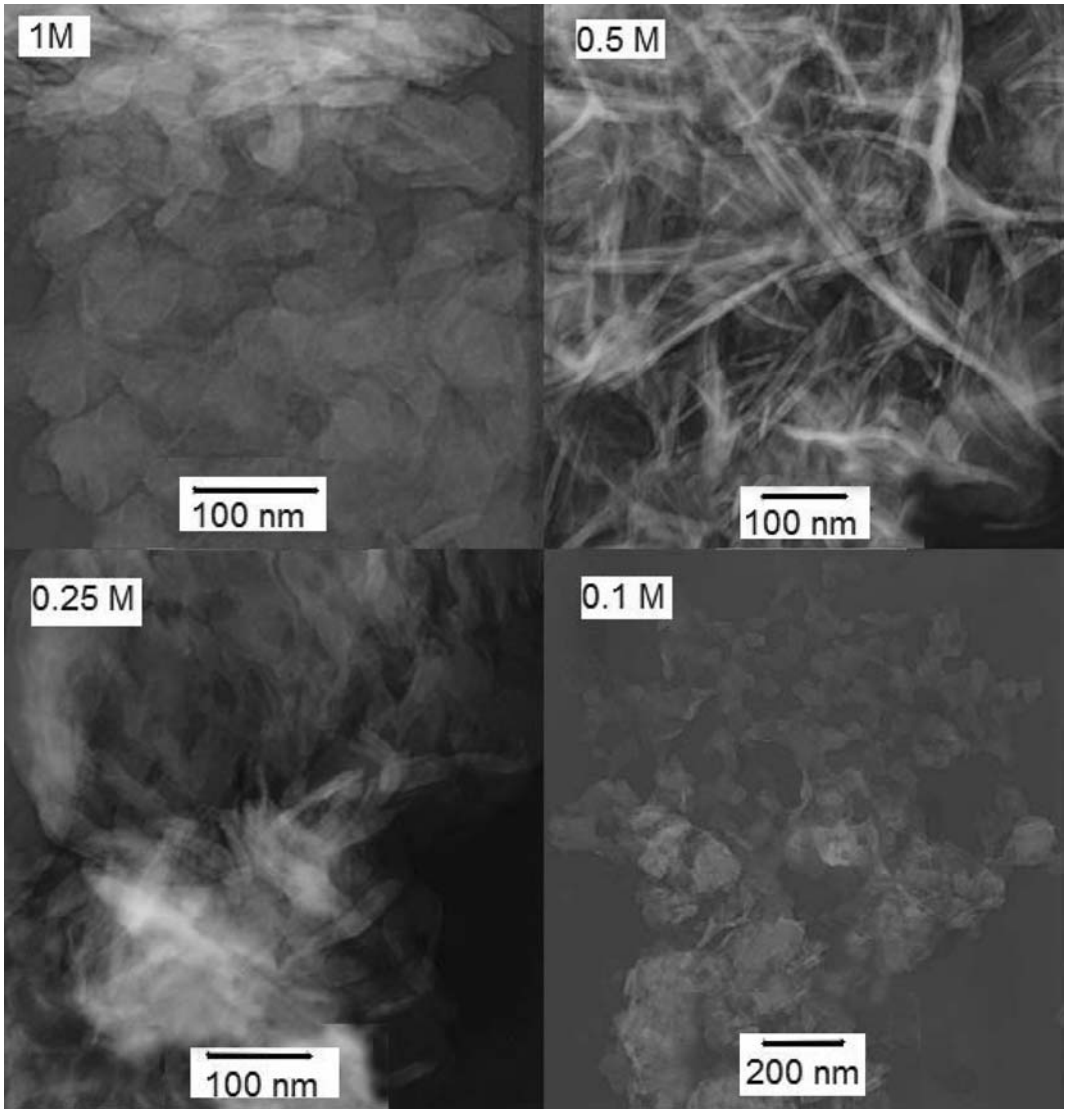

Figure 6. TEM micrographs of Mg/Al-CO_3 LDHs prepared at pH 9 having different molar concentration of NaOH.

varying molar concentration of NaOH. The unusual morphology (figure 6) of LDHs particles was supported the above discussion. However, the exact reason is still unclear and this may be due to the effect of base concentration on the solid solubility of metal hydroxides. Again, in some cases, LDHs platelets tend to form nanorods due to the bigger size/less force in between the platelets and the mechanism was explained in our previous report (Panda *et al* 2008).

Finally, in infrared spectra (figure not provided), the broad peak found at around 3443 cm^{-1} was due to stretching of O–H groups and the bands around 672 cm^{-1} was attributed to the M–O stretching vibration, which remain unchanged for all the cases. Thermal analysis (TGA and DTA) curves for the LDHs prepared in all molar concentration of NaOH provided usual thermal degradation behaviour, i.e. 50–160°C, 170–300°C and 310–450°C, due to loss of water molecules, decomposition of interlayer anions and dehydroxylation of hydroxyl groups which are attached to the metal ions respectively. These results confirmed that the existence of layered structure and NaOH concentration do not affect the internal arrangement of atoms or ions, but significantly influence particle size and morphology.

4. Conclusions

We have prepared the Mg/Al LDHs via the usual co-precipitation method by using sodium hydroxide and the structure was confirmed by using powder X-ray diffraction. Growth study was performed by varying the aging time and pH, and the growth behaviour is qualitatively similar as expected for the Ostwald ripening phenomenon.

In earlier work, sodium hydroxide was used during synthesis for maintaining the pH of the reaction medium. But it has been observed that use of sodium hydroxide significantly lowers the rate of growth, which is qualitatively dissimilar than the well-known growth mechanism. This unexpected behaviour was observed for different pH and it occurs due to the formation of capping layer by Na^+ ions. Finally, this new understanding of the growth process of nano LDHs may be useful for preparing LDH, which may be useful for various future applications.

Acknowledgements

We thank the NanoMission of Department of Science and Technology, India, for supporting this work.

References

Adams J M 1987 *Appl. Clay. Sci.* **2** 309

Adachi-Pagano M, Forano C and Besse J P 2003 *J. Mater. Chem.* **13** 1998

Chang Z, Evans D G, Duan X, Vial C, Ghanbaja J, Prevot V, Roy M and Forano C 2005 *J. Solid State Chem.* **178** 2766

Ennadi A, Legrouri A, Roy A and Besse J P 2000 *J. Mater. Chem.* **10** 2337

Fogg A M, Green V M, Harvey H G and O'Hare D 1999 *Adv. Mater.* **11** 1466

Franklin K R, Lee E and Nunn C C 1995 *J. Mater. Chem.* **5** 565

Hancock M 1990 *Plasticulture* **79** 1439

Hu M and Lei L 2007 *J. Solid State Electrochem.* **11** 847

Kwak S, Kriven W M, Wallig M A and Choy J 2004 *Biomaterials* **25** 5995

Khan A I, Lei L, Norquist A J and O'Hare D 2001 *Chem. Commun.* 2342

Kaneyoshi M and Jones W 1999 *J. Mater. Chem.* **9** 805

Lakraimi M, Legrouri A, Barroug A, Roy A de and Besse J P 2000 *J. Mater. Chem.* **10** 1007

Li F, Wang Y, Yang Q, Evans D G, Forano C and Duan X 2005a *J. Hazardous Mater.* **B125** 89

Li F, Liu X, Yang Q, Liu J, Evans D G and Duan X 2005b *Mater. Res. Bull.* **40** 1244

Panda H S, Srivastava R and Bahadur D 2008a *J. Nanosci. Nanotechnol.* **8** 4218

Panda H S, Srivastava R and Bahadur D 2008b *Mater. Res. Bull.* **43** 1448

Panda H S, Srivastava R and Bahadur D 2009a *J. Phys. Chem.* **B113** 15090

Panda H S, Srivastava R and Bahadur D 2009b *J. Phys. Chem.* **C113** 9560

Prevot V, Casal B and Ruiz-Hitzky E 2001 *J. Mater. Chem.* **11** 554

Talapin D V, Rogach A L, Haase M and Weller H 2001 *J. Phys. Chem.* **B105** 12278

Viswanatha R, Sapra S, Sengupta S, Satpati B, Satym P V, Dev B N and Sarma D D 2004 *J. Phys. Chem.* **B108** 6303

Viswanatha R, Amenitsch H and Sarma D D 2007 *J. Am. Chem. Soc.* **129** 4470

We Q, Olafsen A, Vistad Q B, Roots J and Norby P 2005 *J. Mater. Chem.* **15** 4695

Whilton N T, Vickers P J and Mann S 1997 *J. Mater. Chem.* **7** 1623

Zhang H, Zou K, Sun H and Duan X 2005 *J. Solid State Chem.* **178** 3485

Zhao Y, Li F, Zhang R, Evans D G and Duan X 2002 *Chem. Mater.* **14** 4286